

# Janus Microdroplets with Tunable Self-Recoverable and Switchable Reflective Structural Colors

Mingzhu Liu, Jiemin Fu, Shengsong Yang, Yuchen Wang, Lishuai Jin, So Hee Nah, Yuchong Gao, Yifan Ning, Christopher B. Murray, and Shu Yang\*

Microdroplets made from chiral liquid crystals (CLCs) can display reflective structural colors. However, the small area of reflection and their isotropic shape limit their performance. Here, Janus microdroplets are synthesized through phase separation between CLCs and silicone oil. The as-synthesized Janus microdroplets show primary structural colors with ≈14 times larger area compared to their spherical counterparts at a specific orientation; the orientation and thus the colored/transparent states can be switched by applying a magnetic field. The color of the Janus microdroplets can be tuned ranging from red to violet by varying the concentration of the chiral dopant in the CLC phase. Due to the density difference between the two phases, the Janus microdroplets prefer to orientate the silicone oil side up vertically, enabling the self-recoverable structural color after distortion. The Janus microdroplets can be dispersed in aqueous media to track the configuration and speed of magnetic objects. They can also be patterned as multiplexed labels for data encryption. The magnetic field-responsive Janus CLC microdroplets presented here offer new insights to generate and switch reflective colors with high color saturation. It also paves the way for broader applications of CLCs, including anti-counterfeiting, data encryption, display, and untethered speed sensors.

#### 1. Introduction

Chiral liquid crystals (CLCs)<sup>[1]</sup> that self-organize into helical arrangements can selectively reflect light with a specific range of wavelengths. Compared to the colors generated from dyes and pigments, structural colors<sup>[2]</sup> offer many advantages, such as being fade-resistant, environment-friendly, energy-efficient, long-lasting, and highly stable. More importantly, the colors can be tuned by the change of helical pitch in response to external stimuli, leading to broad applications ranging from dye-free

M. Liu, J. Fu, Y. Wang, L. Jin, S. H. Nah, Y. Gao, C. B. Murray, S. Yang Department of Materials Science and Engineering University of Pennsylvania 3231 Walnut Street, Philadelphia, PA 19104, USA E-mail: shuyang@seas.upenn.edu
S. Yang, Y. Ning, C. B. Murray

S. Yang, Y. Ning, C. B. Murray
Department of Chemistry
University of Pennsylvania
231 S 34th St, Philadelphia, PA 19104, USA

The ORCID identification number(s) for the author(s) of this article can be found under https://doi.org/10.1002/adma.202207985.

DOI: 10.1002/adma.202207985

color coatings,<sup>[3]</sup> stimuli-responsive coloring,<sup>[4]</sup> colorimetric sensors,<sup>[5]</sup> and reflective color displays.<sup>[6]</sup> Typically, CLCs are utilized in the form of thin membranes (thickness < 40  $\mu m)$  by sandwiching them between two parallel substrates with planar LC anchoring.

Taking advantage of the spherical confinement and accessible planar anchoring at the interface, CLC microdroplets are produced with reflective colors, [7] however, with low reflectivity and poor color saturation since light is only reflected from a small spot of the spherical microdroplet surface at a certain viewing angle range. Mechanical stretching or pressing have been implemented to increase the selective Bragg reflection,[8] but the increment is limited. More importantly, mechanical deformation distorts the color appearance. Others have constructed core-shell droplets where the reflection from the interface between CLCs and other phases yields a central spot with concentric rings.<sup>[9]</sup> Nevertheless, the primary reflection area is

not notably amplified. Therefore, creating CLC microdroplets with increased reflection area is highly desired.

Meanwhile, microparticles that can switch between different color modes in a controlled manner are of interest for anti-counterfeiting labels, [10] information storage, [11] displays, [12] and sensors.<sup>[13]</sup> Structural colors have been combined with fluorescent colors to create geminate labels containing two sets of information, [14] however, the short lifetime of fluorescence remains a concern. Janus beads consisting of two different structural colors that can be switched "on" and "off" offer an attractive alternative. Nevertheless, the use of sophisticated triphasic microfluidic devices<sup>[12b,15]</sup> leads to large particle sizes (>100 µm). The conventional emulsion method in combination with the external field-induced alignment of embedded nanoparticles[16] produces microparticles with a broad size distribution, while the layer-by-layer assembly on existing microparticles[17] is challenging to scale up. Janus microparticles can also be generated through phase separation within a spherical microparticle.<sup>[18]</sup> In general, photonic Janus microparticles are assembled from colloidal nanoparticles of different sizes and shapes<sup>[19]</sup> or materials of different refractive indices.<sup>[20]</sup> Again, the color is reflected only from a small area of the microparticle surface. CLC-based Janus microdroplets have been reported.<sup>[13]</sup>

15214055, 2023, 5, Downloaded from https://onlinelibrary.wiley.com/doi/10.1002/adma.202279785 by University of Pennsylvania, Wiley Online Library on [22.05.2023]. See the Terms and Conditions (https://onlinelibrary.wiley.com/terms-and-conditions) on Wiley Online Library for rules of use; OA articles are governed by the applicable Creative Commons Licenseque and Conditions (https://onlinelibrary.wiley.com/terms-and-conditions) on Wiley Online Library for rules of use; OA articles are governed by the applicable Creative Commons Licenseque and Conditions (https://onlinelibrary.wiley.com/terms-and-conditions) on Wiley Online Library for rules of use; OA articles are governed by the applicable Creative Commons Licenseque and Conditions (https://onlinelibrary.wiley.com/terms-and-conditions) on Wiley Online Library for rules of use; OA articles are governed by the applicable Creative Commons Licenseque and Conditions (https://onlinelibrary.wiley.com/terms-and-conditions) on Wiley Online Library for rules of use; OA articles are governed by the applicable Creative Commons Licenseque and Conditions (https://onlinelibrary.wiley.com/terms-and-conditions) on Wiley Online Library for rules of use; OA articles are governed by the applicable Creative Commons Licenseque and Conditions (https://onlinelibrary.wiley.com/terms-and-conditions) on Wiley Online Library for rules of use and the conditions of the cond

However, their photonic properties are not well-studied, nor is the color switchable.

Here, we synthesize Janus microdroplets from CLCs and silicone oil, which phase separate from each other upon removal of their cosolvent, dichloromethane (DCM). When viewing the reflective color generated by CLCs from the silicone oil side, a 14x increase in reflection area compared to that from homogeneous CLC spherical microdroplets is obtained. We attribute this increase to the internal reflection at the curved interface of CLC and silicone oil. The color can be tuned in a broad range by adjusting the concentration of the chiral dopants. Since silicone oil is lighter than CLCs, the Janus microdroplet always orientates with the silicone oil side up vertically, leading to self-recovery of the color when the orientation of the particle is disturbed. To tune the microdroplet orientation, and thus the displayed colors, we incorporate magnetic nanoparticles such that the color displays can be turned on and off by an untethered magnetic field without deforming the droplets. Accordingly, we can track the moving speed of a single magnetic rod by the color pattern. By combining responsive and non-responsive Janus microdroplets, we demonstrate the feasibility of data encryption in different modes.

#### 2. Results and Discussion

#### 2.1. Synthesis of Janus Microdroplets

As shown in Figure 1a, a suspension of spherical microdroplets consisting of CLCs precursors (including chiral LC monomer LC756 (chiral dopant), non-reactive mesogen 5CB, reactive mesogen RM257, and oligomers RM257-1,3 PDT) and silicone oil in DCM are fabricated through a flow-focusing microfluidic device<sup>[21]</sup> and suspended in an aqueous medium. The molecular structures of the chemicals are shown in Figure S1, Supporting Information, and the compositions are listed in Table S1, Supporting Information. Upon removal of DCM, phase separation<sup>[22]</sup> inside the microdroplets occurs, where the silicone oil side appears as the transparent brighter lobe and the CLCs side is the colored darker lobe in the optical microscopy image. The CLC phase is formed due to the satisfaction of: 1) the LC mixture is in the nematic phase at room temperature; 2) the surfactant poly(vinyl alcohol) (PVA, 13-23K, 1.0 wt.% in water) is used in the aqueous solution to enforce a planar anchoring of LCs on the surfaces of microdroplets; and 3) the chiral dopant with desired chemistry and concentration triggers the formation of helical alignment of LCs.

# 2.2. Orientation-Dependent Reflective Color of Janus Microdroplets

CLCs with a certain helical pitch (p) can selectively reflect the light of a specific wavelength  $\lambda$ . According to Bragg's law:  $\lambda = n_{\rm clc} \ p\cos\theta$ , where  $n_{\rm clc}$  is the average refractive index of the CLCs, and  $\theta$  is the angle of incidence with respect to the helix as shown in Figure 1b. In the Janus microdroplets, depending on how light is reflected from different regions of the microdroplets, we could observe different reflective color modes (Figure 1c and Figure S2, Supporting Information). When a

beam of white light is reflected from the CLCs side directly, only the color reflected from the center region can be observed, the same as that of a spherical CLC microdroplet, [7a-d,14] spherical colloidal photonic crystals,[23] and conventional Janus beads<sup>[15a,17]</sup> (see selected examples of each case in Figure S3, Supporting Information). When a beam of white light is reflected from the equator side of the Janus microdroplets, that is, the interface of silicone oil and CLCs, no color is reflected. At the same time, different brightness is observed from the CLCs side versus that from the silicone oil side due to the difference in refractive index. Interestingly, when the white light is reflected from the silicone oil side through the interface, a stripe consisting of concentric colored rings with an area percentage (A)  $\approx$  70% of the whole area is obtained in comparison with A ≈ 5% for a spherical CLC microdroplet, and the color is blue shifted. This dramatic increase of A can be attributed to the internal reflection at the curved silicone oil/CLC interface, as illustrated in Figure 1c and Figure S2, Supporting Information. The curved surface leads to a coupling of the lensing effect of the silicone oil part and the Bragg reflection from the CLC part. The colored pattern changes to concentric rings with alternative colors as the silicone oil and CLC part become increasingly separated (Figure S4, Supporting Information). The dominant color shifts to a slightly longer wavelength when the media of higher refractive indices are used (Figure S5, Supporting Information). Such an effect persists over a broad size range of the Janus microdroplets (diameter of the CLC side, 22, 34, and 45 µm) as shown in Figure S6, Supporting Information. Although light reflected from slightly nonvertical directions may also be collected due to the nonzero numerical aperture (NA = 0.40) of the microscope objective, the increment in reflection area is not significant.

The wavelengths of the structural colors reflected from the microdroplets can be fine-tuned by adjusting the concentration of the chiral dopant, shifting from red ( $\lambda \approx 660$  nm, 3.0 wt.% LC756) to violet ( $\lambda \approx 400$  nm, 5.0 wt.% LC756) as shown in Figure 1c. The color appears blurred near edges due to the light reflection from the background glass slide. By adjusting the weight ratio of silicone oil to CLCs, the curvature of the interface is also changed. Thus, the wavelength of reflected light and the degree of color coverage on the microdroplet vary. Reducing the amount of silicone oil, silicone oil: CLCs = 1:2 wt./wt., leads to the formation of a ring with a shorter wavelength at the outmost of the colored region. Increasing silicone oil: CLCs = 2:1 wt./wt., yields a bright white perimeter due to the total internal reflection[9a,24] (Figure S7, Supporting Information). Thus, silicone oil: CLCs = 1:1 wt./wt. is selected to produce the Janus microdroplets in this study unless otherwise stated.

#### 2.3. Control Experiments

The generation and the thermal stability of the reflected colors are highly dependent on the presence and composition of the oligomers and monomers in CLCs. Without oligomers and monomers, the Janus microdroplets look similar whether viewed from the silicone oil side or the CLCs side (Figure S8a, Supporting Information). This could be attributed to the less

15214095, 2023, 5, Downloaded from https://onlinelibrary.wiley.com/doi/10.1002/adma.202207985 by University Of Pennsylvania, Wiley Online Library on [22.05/2023]. See the Terms

~and-conditions) on Wiley Online Library for rules of use; OA articles are governed by the applicable Creative Commons

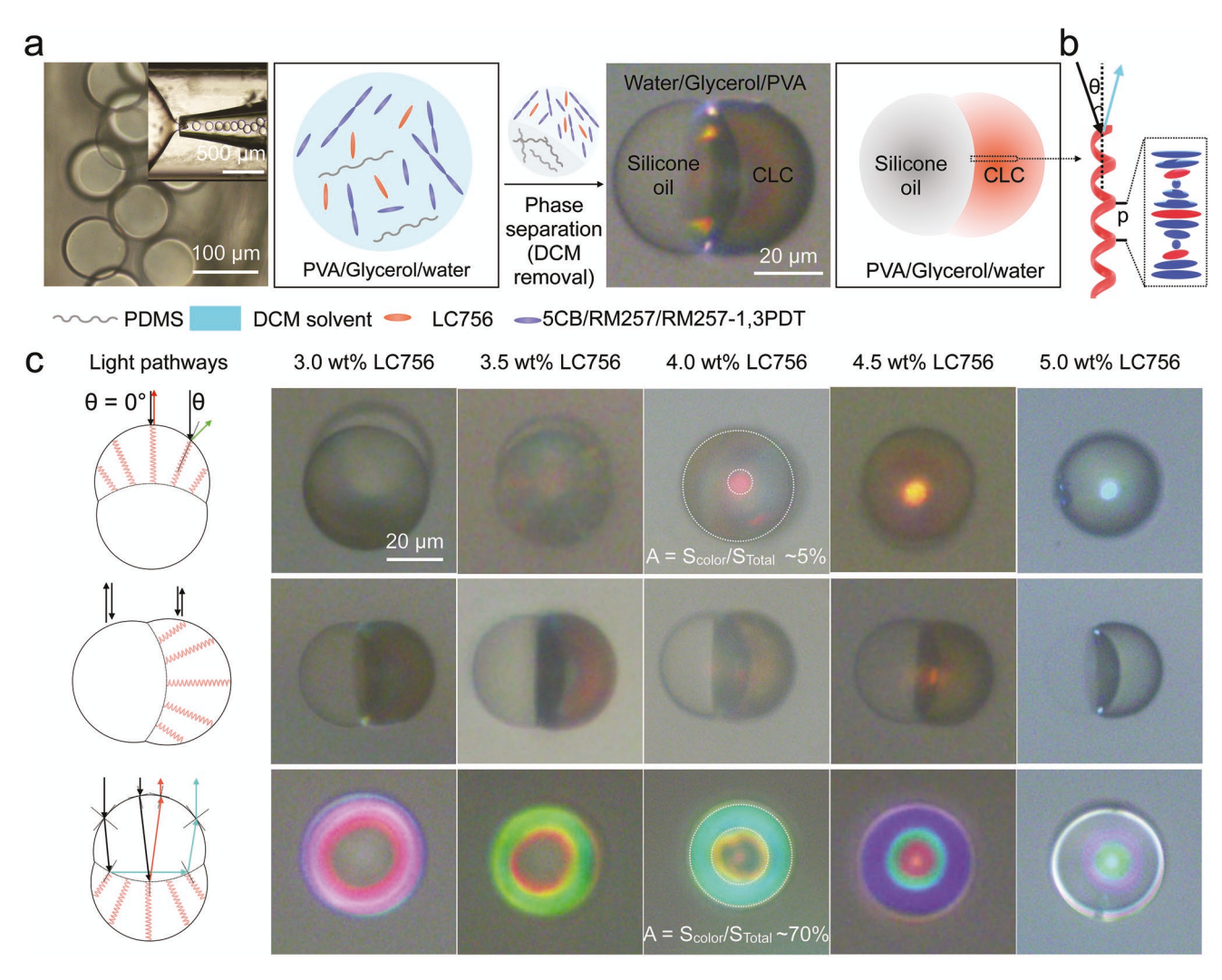


**Figure 1.** Synthesis of Janus microdroplets with orientation-dependent structural color. a) Schematic illustrations and bright field optical microscopy images of the Janus microdroplets synthesized by phase separation of silicone oil and CLCs upon removal of cosolvent DCM. Inset: microdroplets produced via a flow-focusing microfluidic device. b) Schematic illustration of a beam of white light with incident angle  $\theta$  reflected by the CLC helix with pitch p; only a specific color is reflected. c) Schematic illustration and optical microscopy (reflection) images of Janus microdroplets viewed from the CLCs side, the equator side (interface of silicone oil and CLCs), and the silicone oil side, respectively. The LC756 concentration in CLCs is varied while the weight ratio of silicone oil and CLCs is fixed at 1 to 1. The scale bar in (c) applies to all other microscopy images in (c). A is the area percentage of the reflection color.

sharp interfacial curvature between 5CB/LC756 mixture and silicone oil, compared to that of 5CB/LC756 mixed with oligomers and monomers and silicone oil. The structural color disappears near the phase transition temperature ( $T_{\rm NI}$ ) of 5CB,  $\approx 30.0-32.5$  °C (Figure S8b, Supporting Information), while fades at  $\approx 50.0-52.5$  °C when oligomers and monomers are present (Figure S9, Supporting Information). Besides, the density of Janus microdroplets made from silicone oil and 5CB/LC756 is smaller than that of 1.0 wt.% aqueous PVA solution. Thus, the Janus microdroplets will float on a PVA solution but will sink when oligomers and monomers are added in CLCs (density,  $\rho \approx 1.08-1.14$  g mL<sup>-1</sup>, estimated based on the facts that microdroplets with silicone oil: CLCs = 1:1 wt./wt. sink in 10.0 wt.% glycerol in water while floating on 20.0 wt.% glycerol in water).

#### 2.4. Self-Recoverable Color of Janus Microdroplets

Since silicone oil ( $\rho$  = 0.97 g mL<sup>-1</sup>) is lighter than CLCs, the silicone oil side faces up when the microdroplets are dispersed in an aqueous solution (PVA/Glycerol/water mixture with a weight ratio of 1:10:89,  $\rho$  = 1.02 g mL<sup>-1</sup>) and thus showing the circular stripe of structural color as shown in **Figure 2**a,b. The existence of PVA as a surfactant not only preserves the CLC phase, but also prevents the microdroplets from fusion or aggregation together. When the suspension of Janus microdroplets (≈2.0 wt.%) is sandwiched between two glass slides as a smart window, angle-dependent structural colors are observed when illuminated from the top, the silicone oil side (Figure 2c and Figure S10a, Supporting Information). However, when viewed from the bottom of the window, a very weak color is observed

15214055, 2023, 5, Downloaded from https://onlinelibrary.wiley.com/doi/10.1002/adma.202279785 by University of Pennsylvania, Wiley Online Library on [22.05.2023]. See the Terms and Conditions (https://onlinelibrary.wiley.com/terms-and-conditions) on Wiley Online Library for rules of use; OA articles are governed by the applicable Creative Commons Licenseque and Conditions (https://onlinelibrary.wiley.com/terms-and-conditions) on Wiley Online Library for rules of use; OA articles are governed by the applicable Creative Commons Licenseque and Conditions (https://onlinelibrary.wiley.com/terms-and-conditions) on Wiley Online Library for rules of use; OA articles are governed by the applicable Creative Commons Licenseque and Conditions (https://onlinelibrary.wiley.com/terms-and-conditions) on Wiley Online Library for rules of use; OA articles are governed by the applicable Creative Commons Licenseque and Conditions (https://onlinelibrary.wiley.com/terms-and-conditions) on Wiley Online Library for rules of use; OA articles are governed by the applicable Creative Commons Licenseque and Conditions (https://onlinelibrary.wiley.com/terms-and-conditions) on Wiley Online Library for rules of use; OA articles are governed by the applicable Creative Commons Licenseque and Conditions (https://onlinelibrary.wiley.com/terms-and-conditions) on Wiley Online Library for rules of use and the conditions of the cond

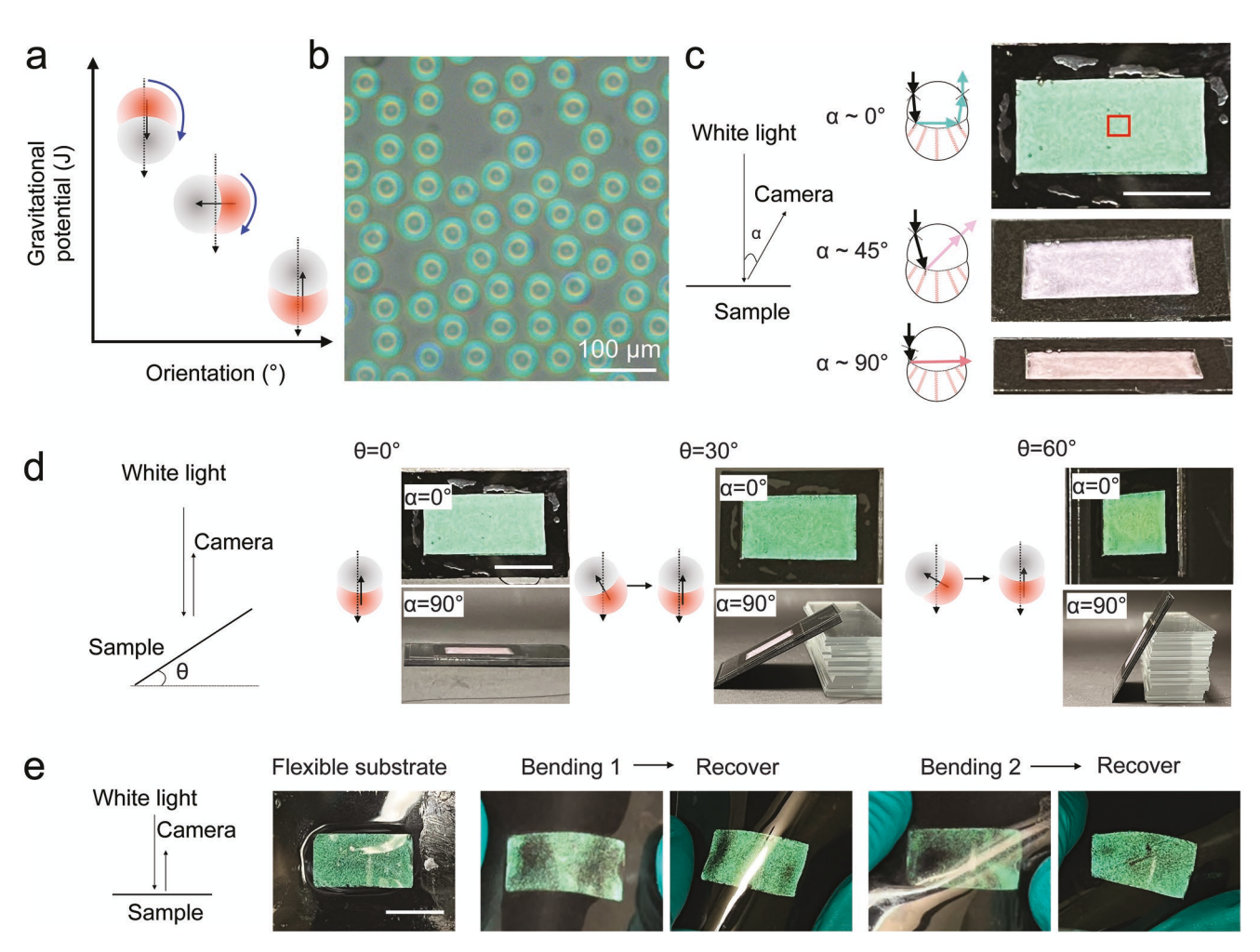


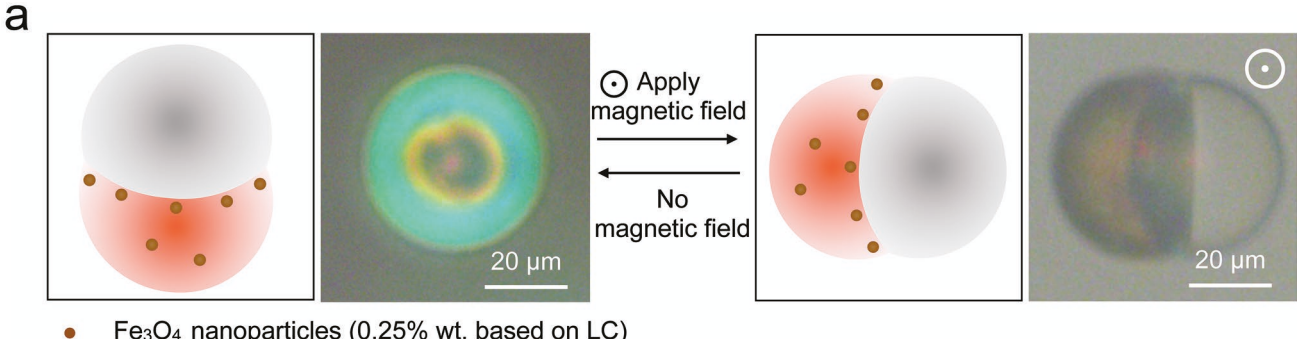
Figure 2. Angle-dependent and self-recoverable color displays. a) Schematic illustrations of the preferred orientation of Janus droplets due to gravitational force and buoyancy force. b) Optical microscopy image (in the reflection mode) of the Janus microdroplets suspended in PVA/Glycerol/water mixture with a weight ratio of 1:10:89. The concentration of LC756, is fixed at 4.0 wt.%. c) Photographs of a display window with the suspension of Janus microdroplets (≈ 2.0 wt.%) sandwiched between two glass slides, showing angle-dependent color. d) Photographs of the display window seen in (c), showing self-recoverable color. e) Photographs of a flexible smart window where the suspension of Janus microdroplets is sandwiched between two PET films. A VHB tape (thickness, 0.8 mm) is used as the spacer. (c–e) Scale bars: 1 cm.

due to the small reflection area of the CLCs surface and the low concentration of the Janus microdroplets in the suspension (Figure S11, Supporting Information). When tilted to different angles, the reflection color first fades due to the reorientation of the microdroplets, followed by recovering within seconds due to the gravitational force (Figure 2d, Movie S1, Supporting Information). Likewise, the self-recoverable microdroplets can be sandwiched between poly(ethylene terephthalate) (PET) films for flexible displays (Figure 2e and Movie S2, Supporting Information).

# 2.5. Magnetic-Responsive Switchable Color

Since the colors reflected from the Janus microdroplets are highly dependent on their orientation, we now exploit the use of a magnetic field to control the orientation of Janus microdroplets for color switching. 0.25 wt.% (vs CLCs) paramagnetic Fe<sub>3</sub>O<sub>4</sub> nanoparticles stabilized by a pro-mesogenic dendritic

ligand (Figure S12, Supporting Information) are introduced to the microdroplets without causing any noticeable color change. As seen in Figure 3a, microdroplets with 4.0 wt.% LC756 lose the colored stripe when they are reoriented under a vertical magnetic field (Figure S10b, Supporting Information), where nanoparticles accumulated at the interface of CLC/silicone oil tend to assemble closer to the magnets. Once the field is removed, the droplets return to their original orientation, and the color recovers within seconds. Optical microscopy images show the synchronous reorientation of microdroplets dispersed in a PVA/Glycerol/water mixture (weight ratio, 1:10:89) under the magnetic field (Figure 3b, Figure S13, and Movie S3, Supporting Information). When the microdroplets are sandwiched between two glass sides, we create colored display windows, where the color, as a function of LC756 concentration, can be switched on and off (Figure 3c and Movie S4, Supporting Information). Further, by spatial control of the application of the magnetic field, we can program color mixing for more advanced color displays (Figure 3d and Movie S5, Supporting



Fe<sub>3</sub>O<sub>4</sub> nanoparticles (0.25% wt. based on LC)

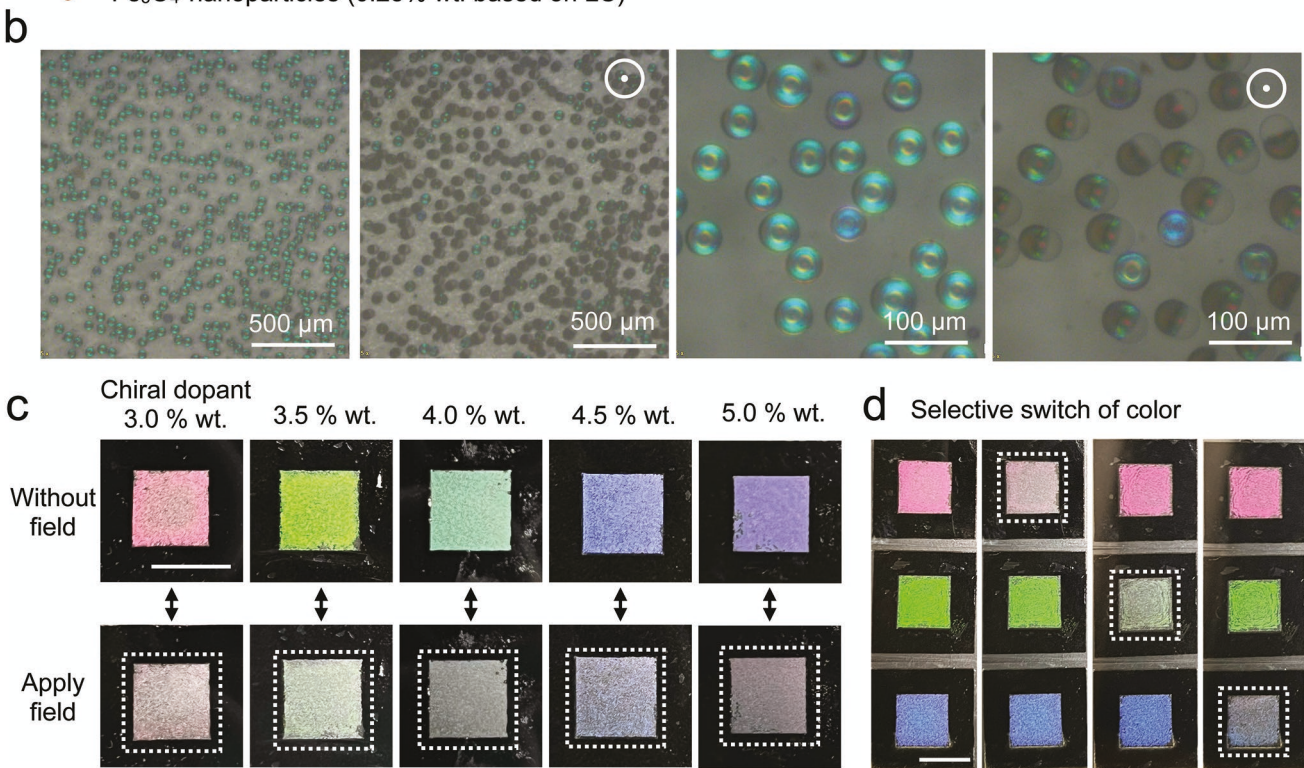


Figure 3. Magnetic field-responsive Janus droplets for switchable color displays. a) Schematic illustrations (left) and optical microscopy image (right, in the reflection mode) showing the magnetic field-induced reorientation of a single Janus droplet suspended in PVA/glycerol/water mixture (weight ratio, 1:10:89). b) Optical microscopy images (in the reflection mode) showing the magnetic field-induced reorientation of the Janus microdroplets suspended in a PVA/glycerol/water mixture. The concentration of the LC756 is 4.0 wt.% for (a,b). c) Photographs of the displays from magnetic fieldresponsive Janus microdroplet suspensions of different LC756 concentrations sandwiched between two glass slides at on (top) and off (bottom) states. d) Photograph of a stripe consisting of three windows with different colored microdroplets, where the windows can be selectively switched off by applying a magnetic field underneath. VHB tape (0.8 mm thick) is used as a spacer. 0.25 wt.% (vs CLCs) paramagnetic Fe<sub>3</sub>O<sub>4</sub> nanoparticles are introduced for all cases. Scale bars: 1 cm in (c,d).

Information). More advanced color mixing with switchable colors can also be achieved by mixing microdroplets with different colors in a suspension and selectively switching off one color as shown in Figure S14, Supporting Information.

# 2.6. Magnetic Sensing and Tracking

The magnetic field-sensitive color change also enables the tracking of magnetic objects. When a magnetic field is applied underneath a tracking pad with sandwiched microdroplets, as shown in Figure 4a, the color-faded regions are consistent with the calculated local magnetic field experienced by the

pad at the plane, demonstrating the ability to sense the morphology of the magnetic objects. Accordingly, we can calculate the moving speed of the magnet based on the pattern generated on the tracking pad (Figure 4b, Figure S15, and Movie S6, Supporting Information). When the magnet moves at a speed (e.g.,  $4 \text{ mm s}^{-1}$ ) faster than the droplet recovery speed, a pattern with a long tail is obtained, recording the moving path.

## 2.7. Data Encryption

The magnetic field-induced on/off color switch makes the microdroplets potential inks for data encryption. We design a www.advancedsciencenews.com

www.advmat.de

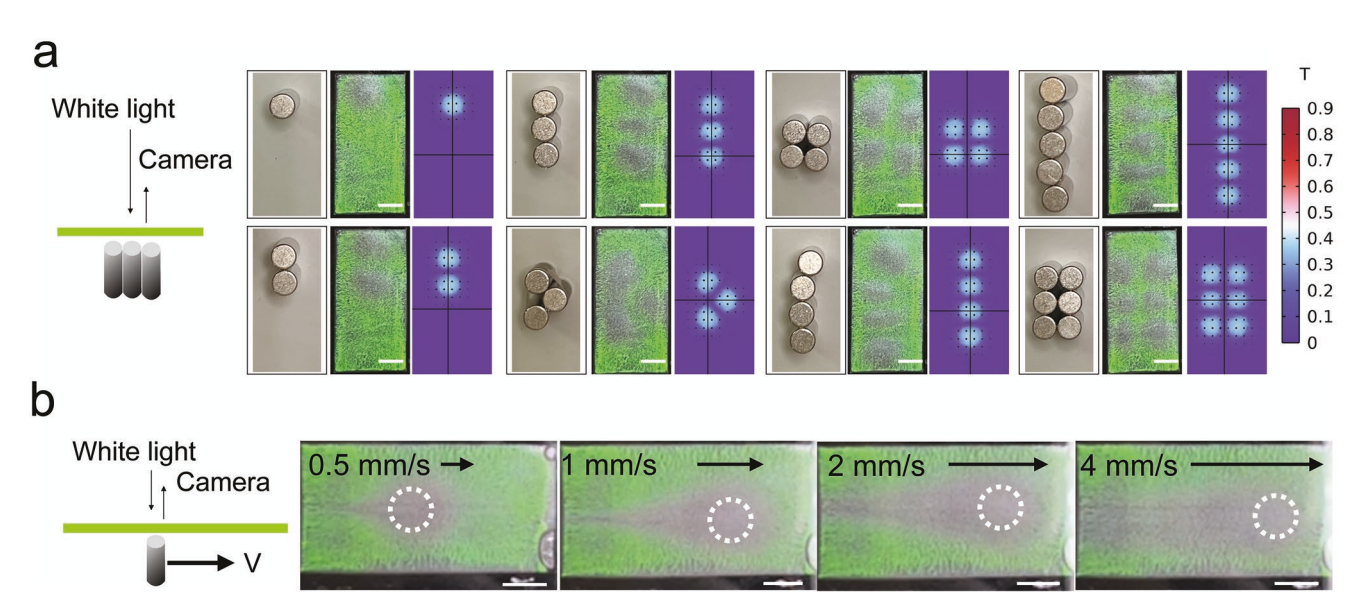
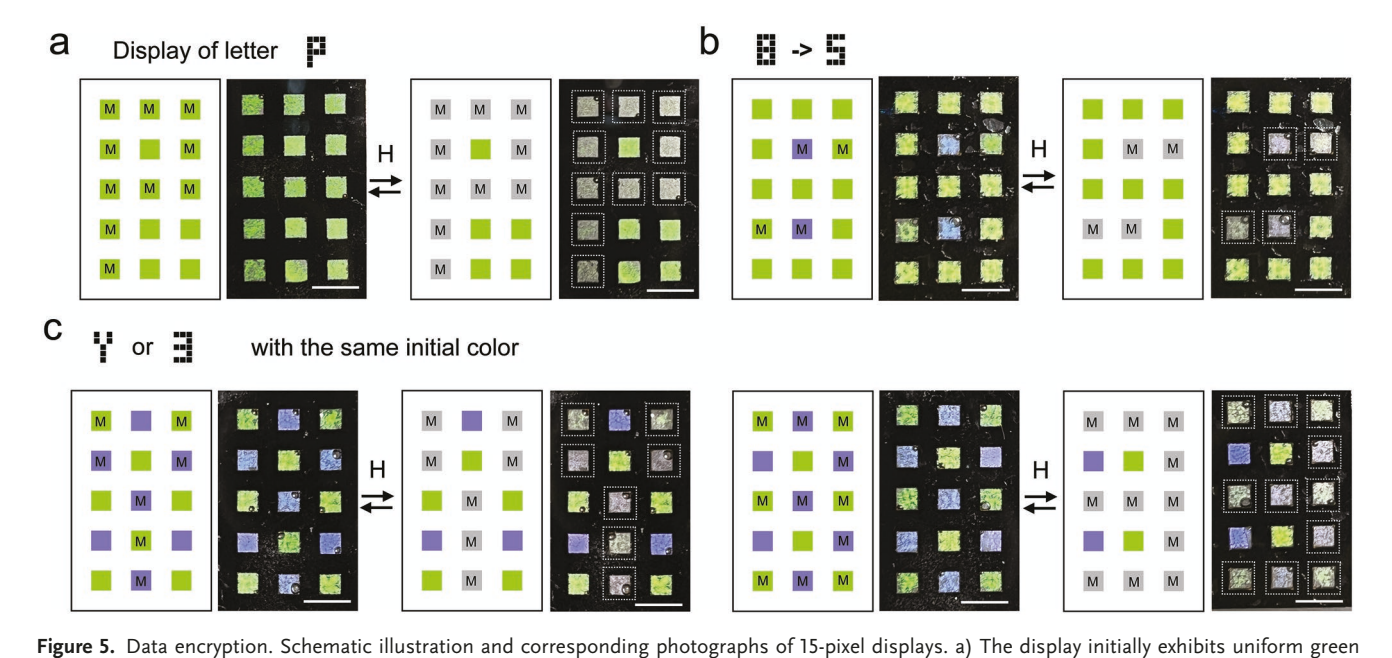


Figure 4. A magnetic tracking pad. a) Left, schematic illustration of the side view of the tacking pad with magnetic rods underneath. Right, photographs of the standing magnetic rods, the corresponding tracking pad, and the magnetic field in the Z direction simulated by COMSOL when different numbers or different configurations of magnetic rods are used. b) Left, schematic illustration of the side view of the tracking pad with a magnetic rod moving underneath. Right, photographs of the tracking pad. The arrow indicates the moving direction, the line length represents the speed, and the dotted circle indicates the position of the magnetic rod underneath. The microdroplets contain 3.5 wt.% LC756 and 0.25 wt.% magnetic nanoparticles on the CLCs side. 0.8 mm thick VHB tape is used as the spacer. Scale bars: 5 mm.

15-pixel label where the reflective structure color and magnetic responsiveness of the Janus microdroplets in each pixel can be programmed separately by choosing the proper suspension. Different data encryption-decryption modes can be designed. **Figure 5**a and Movie S7, Supporting Information, show the label, which initially reflects a uniform color with microdroplets

containing 3.5 wt.% LC756, revealing the letter "P" when a magnetic field is applied to switch off the color. By combining Janus microdroplets with 3.5 wt.% and 4.5 wt.% LC756, we can switch the display from a colored number "8" to a colored number "5" when designated pixels are switched off (Figure 5b and Movie S8, Supporting Information). Distinct information



colors but shows the letter "P" when the magnetic field is applied. b) The display initially exhibits "8" and switches to the number "5" when the magnetic field is applied. c) The display initially does not exhibit anything but shows the letter "Y" or number "3" depending on the programming process when the magnetic field is applied. M in the schemes denotes the magnetic field-responsive Janus microdroplets (with 0.25 wt.% magnetic nanoparticles). The green and purple Janus microdroplets contain 3.5 wt.% and 4.5 wt.% LC756 on the CLCs side, respectively. 0.8 mm thick VHB tape is used as the spacer. Scale bars: 5 mm.

15214055, 2023, 5, Downloaded from https://onlinelibrary.wiley.com/doi/10.1002/adma.202279785 by University of Pennsylvania, Wiley Online Library on [22.05.2023]. See the Terms and Conditions (https://onlinelibrary.wiley.com/terms-and-conditions) on Wiley Online Library for rules of use; OA articles are governed by the applicable Creative Commons Licenseque and Conditions (https://onlinelibrary.wiley.com/terms-and-conditions) on Wiley Online Library for rules of use; OA articles are governed by the applicable Creative Commons Licenseque and Conditions (https://onlinelibrary.wiley.com/terms-and-conditions) on Wiley Online Library for rules of use; OA articles are governed by the applicable Creative Commons Licenseque and Conditions (https://onlinelibrary.wiley.com/terms-and-conditions) on Wiley Online Library for rules of use; OA articles are governed by the applicable Creative Commons Licenseque and Conditions (https://onlinelibrary.wiley.com/terms-and-conditions) on Wiley Online Library for rules of use; OA articles are governed by the applicable Creative Commons Licenseque and Conditions (https://onlinelibrary.wiley.com/terms-and-conditions) on Wiley Online Library for rules of use; OA articles are governed by the applicable Creative Commons Licenseque and Conditions (https://onlinelibrary.wiley.com/terms-and-conditions) on Wiley Online Library for rules of use and the conditions of the cond

can be encoded into the initial states with the same-colored information. For example, two labels of alternating-colored pixels containing 3.5 and 4.5 wt.% LC756, respectively, appear the same at the initial state. However, depending on how the magnetic-responsive pixels are arranged, they can letter "Y" or number "3", separately (Figure 5c, Movie S9, Supporting Information). The data encrypted can be programmed by the initial color and magnetic responsiveness of each pixel, proving a robust strategy in data encryption for applications in switchable color display and anti-counterfeiting.

# 3. Conclusion

Janus microdroplets consisting of CLCs and silicone oil are synthesized, displaying a much larger area of tunable reflective structural color than the conventional spherical CLC microdroplets. Our Janus microdroplets prefer the orientation where the silicone oil side faces upwards due to gravity, thus, the displayed color can self-recover within seconds to the original one after being tilted or bent. Incorporating magnetic nanoparticles into the Janus microdroplets allows for remotely switching on and off the structural colors under the magnetic field. When the magnetic rods are placed underneath a tracking pad made of suspended, magnetic field-responsive Janus microdroplets, the configuration of multiple rods and the moving speed of a single rod can be predicted from the pattern shown on the pad. Combining the Janus microdroplets with and without magnetic nanoparticles, we fabricate 15-pixel labels for the encryption and decryption of information. Our Janus microdroplets open a new gate in using the structural colors of CLCs for applications ranging from display, anti-counterfeiting, to information encryption.

# 4. Experimental Section

Materials: 4'-pentyl-4-biphenylcarbonitrile(5CB) and 1,4-bis-[4-(3acryloyloxy-proplyoxy) benzoyloxy]-2-methylbenzene (RM257, > 95%) were purchased from Wilshire Technologies Inc. and used as received. (3R,3aR,6S,6aR)-hexahydrofuro[3,2-b]furan-3,6-diyl dopant bis (4-((4-(((4-(acryloyloxy)butoxy)carbonyl)oxy)benzoyl)oxy)benzoate) (Paliocolor LC 756) was purchased from Hunan ChemFish Scientific Co. Poly(vinyl alcohol) (PVA, 13-23k, 87-89% hydrolyzed), 1,3-propanedithiol (1,3-PDT, >99%), silicone oil (viscosity 1000 cSt), DCM (HPLC grade, 99.9%), chloroform (CHCl<sub>3</sub>, anhydrous, ≥ 99%), hexane (anhydrous, 95%), isopropanol (anhydrous, 99.5%), methanol (anhydrous, 99.8%), Iron(0) pentacarbonyl (Fe(CO)<sub>5</sub>, >99.99%), oleylamine (technical grade, 70%), and oleic acid (technical grade, 90%) were purchased from Sigma-Aldrich and used as received. 1-octadecene (technical grade, 90%) was purchased from Acros Organics. Triton X-100 was purchased from Alfa Aesar. Black double-sided acrylic very high bond (VHB) tape (BA 250, thickness of 800 μm) was purchased from 3M. Glass cover slides of 25 mm x 25 mm or 22 mm x 50 mm were purchased from Fisher Scientific and used as received. Clear PET Films were purchased from Professional Plastics and used as received. Magnets (rod shape with thickness of 0.25 inches and diameter of 1, 1.5, or 2 inches, and smaller rods with height of 1 inch and diameter of 0.25 inches, grade N42) were purchased from Amazing Magnets.

Synthesis and Functionalization of  $Fe_3O_4$  Nanoparticles:  $Fe_3O_4$  nanoparticles were synthesized via a thermal-decomposition method. [25] 10 mL of 1-octadecene, 3 mL of oleylamine, and 4 mL of oleic acid were degassed with stirring under vacuum at 120 °C for 30 min. Then the

flask was purged with nitrogen and the temperature was ramped to 330 °C with a ramping rate of 30 °C min<sup>-1</sup> and kept for one hour. At 150 °C, 100  $\mu$ L of Fe(CO)<sub>5</sub> was injected swiftly. The color of the solution turned from yellow to black, representing the formation of colloidal Fe<sub>2</sub>O<sub>4</sub> nanoparticles. The reaction suspension was cooled down to room temperature, and isopropanol was used as an antisolvent for size-selective precipitation. Nanoparticles with a diameter of  $\approx$  30 nm were collected and dispersed in hexane to make a suspension with a concentration of 10 mg mL<sup>-1</sup>. Promesogenic ligands were synthesized following a reported procedure. [26] Then 10 mg of promesogenic ligands were dissolved in 4 mL of chloroform, followed by adding 1 mL of Fe<sub>3</sub>O<sub>4</sub> suspension with vigorous stirring. The scintillation vial was sealed and kept at 50 °C for 12 h. 10 mL of methanol was added as an antisolvent to precipitate the nanoparticles, and the suspension was then centrifuged. The sediments were washed two more times with methanol to completely remove extra ligands and redispersed in DCM, making a suspension with a concentration of 10 mg mL<sup>-1</sup>. The nanoparticles can be dispersed stably in the organic precursor used to synthesize Janus microdroplets after the ligand exchange.

Synthesis of Janus Microdroplets: A flow-focusing microcapillary<sup>[21]</sup> was used for the fabrication of microdroplets. The diameter of the inner capillary orifices was about 200 µm. The aqueous phase was 1:1 wt:wt Glycerol: 5% PVA, and the outer phase was a precursor solution consisting of LC monomer RM257, LC oligomer (RM257-1,3 PDT) synthesized following the literature, [27] 5CB, chiral dopant (LC756, 3.0-5.0 wt.% based on the total weight of monomer, oligomer, and 5CB), silicone oil, and Fe<sub>3</sub>O<sub>4</sub> nanoparticle (0.25 wt.% based on the total weight of LCs when applicable) in DCM (see Table S1, Supporting Information, for compositions of different microdroplets). The solution was diluted with DCM to create sub-100 µm microdroplets (Figure S6, Supporting Information). The solution was sonicated in a sonication bath for 2 min before being added to a syringe for microdroplets generation. The typical flow speeds were 300  $\mu$ L h<sup>-1</sup> for the inner phase and 2000 µL h<sup>-1</sup> for the outer phase to generate microdroplets with a diameter of 90  $\mu m$ . Microdroplets were collected in 20 mL vials with 10 mL solution of PVA: glycerol: water with a weight ratio of 1:10:89. After the microdroplets were collected, the vials suspended in PVA/ water/glycerol solution were placed onto the heating plate uncapped at 65 °C for 4 h with gentle shaking every several hours to promote the evaporation of DCM and prevent particles from sticking onto the bottom surface of the vial. After DCM removal, the suspension was cooled at room temperature and allowed to sit on top of a magnet overnight to enhance the magnetic response. Janus microdroplets with a size (diameter of the CLC side) around 45 µm were produced and used for further studies. Janus microdroplets were concentrated to ≈ 2.0 wt.% for the fabrication of display windows. To tune the curvature of the silicone oil part and the CLC part, and thus, the interface geometry, triton X-100 solution (0.2 wt.% in PVA: glycerol: water with a weight ratio of 1:10:89) was added to the microdroplets suspension. The suspension was heated inside a 60 °C oven and cooled at room temperature overnight before observation.

Fabrication of the Colored Displays: The displays were fabricated by sandwiching the VHB tape (3 M BA250) with opening areas as a spacer in between two pieces of glass slides or PET films. The VHB tapes were cut with a laser cutter (Universal Laser System PLS4.75) to create openings in designated areas (1 cm x 2 cm for Figure 2, 1 cm x 1 cm for Figure 3, 1.5 cm x 3 cm for Figure 4a,b, and patterned squares of 3 mm x 3 mm with a spacing distance of 3 mm for the 15-pixel labels for Figure 5a-5c). In detail, the spacer was attached to one piece of glass (or PET film), then the suspension of the Janus microdroplets (≈ 2.0 wt.%) in water/PVA/glycerol was added into the opening areas of the spacer. Following that, another piece of the glass (or PET film) was carefully placed on top without generating bubbles. The fabricated displays were then used for further studies. For the patterned displays used to demonstrate data encryptions, different suspensions of Janus microdroplets (different reflective colors generated by microdroplets with 3.5 or 4.5 wt.% LC756, with and without 0.25 wt.% magnetic nanoparticles, respectively) were added to designated areas. For the

15214055, 2023, 5, Downloaded from https://onlinelibrary.wiley.com/doi/10.1002/adma.202279785 by University of Pennsylvania, Wiley Online Library on [22.05.2023]. See the Terms and Conditions (https://onlinelibrary.wiley.com/terms-and-conditions) on Wiley Online Library for rules of use; OA articles are governed by the applicable Creative Commons Licenseque and Conditions (https://onlinelibrary.wiley.com/terms-and-conditions) on Wiley Online Library for rules of use; OA articles are governed by the applicable Creative Commons Licenseque and Conditions (https://onlinelibrary.wiley.com/terms-and-conditions) on Wiley Online Library for rules of use; OA articles are governed by the applicable Creative Commons Licenseque and Conditions (https://onlinelibrary.wiley.com/terms-and-conditions) on Wiley Online Library for rules of use; OA articles are governed by the applicable Creative Commons Licenseque and Conditions (https://onlinelibrary.wiley.com/terms-and-conditions) on Wiley Online Library for rules of use; OA articles are governed by the applicable Creative Commons Licenseque and Conditions (https://onlinelibrary.wiley.com/terms-and-conditions) on Wiley Online Library for rules of use; OA articles are governed by the applicable Creative Commons Licenseque and Conditions (https://onlinelibrary.wiley.com/terms-and-conditions) on Wiley Online Library for rules of use and the conditions of the cond

fabrication of the tracking pad used to sense the local magnetic field and track the moving magnet, a suspension of microdroplets containing 3.5 wt.% LC756 and 0.25 wt.% magnetic nanoparticles was used.

Characterization: Bright-field and reflection microscopy images and movies were obtained using an Olympus BX61 Motorized Microscope. The reflective color change with temperature was monitored with a microscope (Zeiss, Axio imager.M2m) equipped with a thermal stage (Linkam Scientific Instruments Ltd., LTS420) with a heating/cooling rate at 10 °C min<sup>-1</sup> and held at a certain temperature for 5 min. The transmission electron microscope (TEM) image of Fe<sub>3</sub>O<sub>4</sub> nanoparticles was taken on a JEOL JEM-1400 at 120 kV. The magnetic field generated by the magnets was calculated using the commercial finite element package COMSOL Multiphysics 5.4 in the AC/DC module. In the simulations, the magnetization parameter of 900 kA m<sup>-1</sup> was used. The speed of the moving magnet used for Figure 4b was controlled using an LTS300-300 mm translation stage (Thorlabs, Inc.). The photographs of samples were taken with an iPhone camera. Some images were digitally post-processed to improve brightness and contrast.

# **Supporting Information**

Supporting Information is available from the Wiley Online Library or from the author.

### Acknowledgements

The authors acknowledge Professor Daeyeon Lee for the use of instruments for microfluidic device fabrication. Dr. Baohong Chen and Professor Arjun Yodh are acknowledged for helpful discussions. This work was supported by National Science Foundation (NSF) through the Materials Research Science and Engineering Center at the University of Pennsylvania (DMR-1720530). Shengsong.Y. and C.B.M. acknowledge the support from the Office of Naval Research (ONR) Multidisciplinary University Research Initiative Award N00014-18-1-2497. C.B.M. acknowledges the Richard Perry University Professorship at the University of Pennsylvania.

# **Conflict of Interest**

The authors declare no conflict of interest.

#### **Author Contributions**

M.L. and Shu.Y. conceived the concept; M.L. led the experiments and prepared the samples with the help of J.F., Y.W., L.J., S.N., and Y.G.; Shengsong.Y. and Y.N. synthesized the magnetic nanoparticles under C.B.M.'s supervision. M.L., J.F., and Shu.Y. wrote the manuscript; all authors discussed the results and reviewed the manuscript.

#### **Data Availability Statement**

The data that support the findings of this study are available in the supplementary material of this article.

### **Keywords**

cholesteric liquid crystals, data encryption, Janus microdroplets, reflective structural color displays, switchable

Received: August 31, 2022 Revised: October 12, 2022 Published online: December 18, 2022

- [1] a) H. K. Bisoyi, T. J. Bunning, Q. Li, Adv. Mater. 2018, 30, 1706512;
   b) H. K. Bisoyi, Q. Li, Chem. Rev. 2022, 122, 4887;
   c) L. Wang, A. M. Urbas, Q. Li, Adv. Mater. 2020, 32, 1801335.
- [2] B. Datta, E. F. Spero, F. J. Martin-Martinez, C. Ortiz, Adv. Mater. 2022, 34, 2100939.
- [3] D.-Y. Kim, K. M. Lee, T. J. White, K.-U. Jeong, NPG Asia Mater. 2018, 10, 1061
- [4] a) S. U. Kim, Y. J. Lee, J. Liu, D. S. Kim, H. Wang, S. Yang, Nat. Mater. 2022, 21, 41; b) A. Ryabchun, F. Lancia, J. Chen, D. Morozov, B. L. Feringa, N. Katsonis, Adv. Mater. 2020, 32, 2004420.
- [5] a) A. M. Martinez, M. K. Mcbride, T. J. White, C. N. Bowman, Adv. Funct. Mater. 2020, 30, 2003150; b) J. Ma, Y. Yang, C. Valenzuela, X. Zhang, L. Wang, W. Feng, Angew. Chem., Int. Ed. 2022, 61, 202116219; c) D. J. Mulder, A. P. H. J. Schenning, C. W. M. Bastiaansen, J. Mater. Chem. C 2014, 2, 6695; d) R. Moreddu, M. Elsherif, H. Butt, D. Vigolo, A. K. Yetisen, RSC Adv. 2019, 9, 11433.
- [6] a) J. Li, H. K. Bisoyi, J. Tian, J. Guo, Q. Li, Adv. Mater. 2019, 31, 1807751; b) S. Cui, L. Qin, X. Liu, Y. Yu, Adv. Opt. Mater. 2022, 10, 2102108; c) Y. Li, D. Luo, Z. H. Peng, Opt. Mater. Express 2016, 7, 16.
- [7] a) S. S. Lee, S. K. Kim, J. C. Won, Y. H. Kim, S. H. Kim, Angew. Chem., Int. Ed. 2015, 54, 15266; b) R. Qu, T. F. George, G. Li, J. Mater. Chem. C 2022, 10, 413; c) K. G. Noh, S. Y. Park, Mater. Horiz. 2017, 4, 633; d) Y. J. Kim, S. Y. Park, ACS Appl. Mater. Interfaces 2020, 12, 47342; e) C. Yang, B. Wu, J. Ruan, P. Zhao, L. Chen, D. Chen, F. Ye, Adv. Mater. 2021, 33, 2006361; f) J. Fan, Y. Li, H. K. Bisoyi, R. S. Zola, D. K. Yang, T. J. Bunning, D. A. Weitz, Q. Li, Angew. Chem., Int. Ed. 2015, 54, 2160; g) H. J. Seo, S. S. Lee, J. Noh, J.-W. Ka, J. C. Won, C. Park, S.-H. Kim, Y. H. Kim, J. Mater. Chem. C 2017, 5, 7567.
- [8] a) C. J. Yang, B. H. Wu, J. Ruan, P. Zhao, J. Z. Shan, R. Zhang, D. K. Yoon, D. Chen, K. Liu, ACS Appl. Polym. Mater. 2022, 4, 463;
  b) J.-S. Lim, Y.-J. Kim, S.-Y. Park, Sens. Actuators, B 2021, 329, 129165;
  c) S. S. Lee, J. B. Kim, Y. H. Kim, S. H. Kim, Sci. Adv. 2018, 4, eaat8276.
- [9] a) Y. Geng, J.-H. Jang, K.-G. Noh, J. Noh, J. P. F. Lagerwall, S.-Y. Park, Adv. Opt. Mater. 2018, 6, 1700923; b) S. S. Lee, H. J. Seo, Y. H. Kim, S. H. Kim, Adv. Mater. 2017, 29, 1606894; c) M. Schwartz, G. Lenzini, Y. Geng, P. B. Ronne, P. Y. A. Ryan, J. P. F. Lagerwall, Adv. Mater. 2018, 30, 1707382.
- [10] a) W. Ren, G. Lin, C. Clarke, J. Zhou, D. Jin, Adv. Mater. 2020, 32, 1901430; b) W. Hong, Z. Yuan, X. Chen, Small 2020, 16, 1907626.
- [11] Y. Sun, X. Le, S. Zhou, T. Chen, Adv. Mater. 2022, 2201262.
- [12] a) Y. Komazaki, H. Hirama, T. Torii, J. Appl. Phys. 2015, 117, 154506;
   b) H. Wang, S. Yang, S. N. Yin, L. Chen, S. Chen, ACS Appl. Mater. Interfaces 2015, 7, 8827.
- [13] A. Concellon, D. Fong, T. M. Swager, J. Am. Chem. Soc. 2021, 143, 9177.
- [14] L. Qin, X. Liu, K. He, G. Yu, H. Yuan, M. Xu, F. Li, Y. Yu, Nat. Commun. 2021, 12, 699.
- [15] a) S. K. Nam, J. B. Kim, S. H. Han, S. H. Kim, ACS Nano 2020, 14, 15714; b) S. S. Liu, C. F. Wang, X. Q. Wang, J. Zhang, Y. Tian, S. N. Yin, S. Chen, J. Mater. Chem. C 2014, 2, 9431.
- [16] J. Ge, H. Lee, L. He, J. Kim, Z. Lu, H. Kim, J. Goebl, S. Kwon, Y. Yin, J. Am. Chem. Soc. 2009, 131, 15687.
- [17] S. Y. Lee, J. Choi, J. R. Jeong, J. H. Shin, S. H. Kim, Adv. Mater. 2017, 29, 1605450.
- [18] a) L. Cai, F. Bian, H. Chen, J. Guo, Y. Wang, Y. Zhao, Chem 2021, 7, 93; b) T. Lu, E. Spruijt, J. Am. Chem. Soc. 2020, 142, 2905.
- [19] M. Xiao, J. Liu, Z. Chen, W. Liu, C. Zhang, Y. Yu, C. Li, L. He, J. Mater. Chem. C 2021, 9, 11788.
- [20] H. Wang, Y. Liu, Z. Chen, L. Sun, Y. Zhao, Sci. Adv. 2020, 6, eaay1438.
- [21] A. S. Utada, L. Y. Chu, A. Fernandez-Nieves, D. R. Link, C. Holtze, D. A. Weitz, MRS Bull. 2011, 32, 702.
- [22] a) J. Jeong, A. Gross, W. S. Wei, F. Tu, D. Lee, P. J. Collings, A. G. Yodh, Soft Matter 2015, 11, 6747; b) N. Gogibus, U. Maschke,

15214095, 2023, 5, Downloaded from https://onlinelibrary.wiley.com/doi/10.1002/adma.202207985 by University Of Pennsylvania, Wiley Online Library on [22.05/2023]. See the Terms

and-conditions) on Wiley Online Library for rules of use; OA articles are governed by the applicable Creative Commons License

- F. Benmouna, B. Ewen, X. Coqueret, M. Benmouna, J. Polym. Sci., Part B: Polym. Phys. 2001, 39, 581.
- [23] a) Y. Zhao, L. Shang, Y. Cheng, Z. Gu, Acc. Chem. Res. 2014, 47, 3632; b) N. Vogel, S. Utech, G. T. England, T. Shirman, K. R. Phillips, N. Koay, I. B. Burgess, M. Kolle, D. A. Weitz, J. Aizenberg, Proc. Natl. Acad. Sci. U. S. A. 2015, 112, 10845; c) R. Ohnuki, M. Sakai, Y. Takeoka, S. Yoshioka, Langmuir 2020, 36, 5579.
- [24] A. E. Goodling, S. Nagelberg, B. Kaehr, C. H. Meredith, S. I. Cheon, A. P. Saunders, M. Kolle, L. D. Zarzar, *Nature* **2019**, *566*, 523.
- [25] L. Qiao, Z. Fu, J. Li, J. Ghosen, M. Zeng, J. Stebbins, P. N. Prasad, M. T. Swihart, ACS Nano 2017, 11, 6370.
- [26] Y. Ning, S. Yang, Z. Liu, Y. Morimitsu, C. Osuji, C. B. Murray, unpublished.
- [27] Y. Xia, X. Zhang, S. Yang, Angew. Chem., Int. Ed. 2018, 57, 5665.